Energy-Efficient Resilience in Translucent Optical Networks With Mixed Regenerator Placement

Xiaoliang Chen, Fan Ji, Yanan Wu, and Zuqing Zhu

***Abstract*—In this paper, we investigate energy-efficient resilience designs for the translucent optical networks using mixed regenerator placement (MRP). We consider both static and dynamic traffic scenarios and aim to provide 100% restoration against single-link failures while minimizing the total energy-cost on regenerators. For static traffic scenarios, we formulate an integer linear programming (ILP) model to solve the energy-efficient *p*-cycle design for translucent optical networks with MRP. The ILP model optimizes the allocation of working and protection resources jointly under the quality of transmission constraint, with the objective to minimize the total energy cost. A heuristic that can sequentially optimize the *p*-cycle designs for connections is proposed afterward. We use simulations to evaluate the performance of the algorithms with both uniform and nonuniform traffic models. For dynamic traffic scenarios, we design an algorithm that can handle the setting-up and tearing-down of *p*-cycles dynamically, according to the time-variant connections. We enhance this algorithm by introducing a reoptimization procedure, which can reassemble existing *p*-cycles for higher energy efficiency. An ILP model is formulated and solved for the *p*-cycle reoptimization. We then consider two reoptimization scenarios: (1) on demand (*p*-cycle-oDRO) and (2) on schedule (*p*-cycle-oSRO). In addition to the link-based *p*-cycle, we also study the path-based shared backup path protection scheme.**

***Index Terms*—Mixed regenerator placement (MRP); *p*-cycle; *p*-cycle reoptimization; Shared backup path protection (SBPP); Translucent optical networks.**

I. Introduction

Recent research indicates that Internet traffic has been growing exponentially with an annual rate of more than 34% [1]. With their tremendous bandwidth, optical fibers make optical networks the only feasible infrastructure known so far that can adapt to the consequent bandwidth-demand increases, especially for metro and core networks. Today's optical networks rely on wavelength-division multiplexing (WDM) transponders to transmit optical signals, and they use wavelength cross-connect switches to route signals along the lightpaths. Depending on how the optical signals are handled in lightpaths, optical networks have been categorized as transparent, translucent, and opaque. In transparent optical networks, an optical signal bypasses all optical–electronic–optical (O/E/O) conversions at the intermediate nodes along its lightpath. As transmission impairments can accumulate along transparent lightpaths, it is difficult in practice to deploy transparent optical networks on a large scale [2]. It is known that O/E/O reamplification, reshaping, and retiming (3R) regenerators can improve the quality of transmission (QoT) dramatically [3]. However, O/E/O 3R regenerators usually incur additional capital and operational expenditures owing to their relatively high equipment cost and power consumption. Therefore, the opaque optical networks that make optical signals experience O/E/O 3R regenerators at every intermediate node are also not promising for practical deployment. With the idea of placing O/E/O 3R regenerators sparsely, Ramamurthy *et al.* proposed to use translucent optical networks for better cost effectiveness [2].

Previously, all-optical reamplification and reshaping (2R) regenerators have been experimentally demonstrated for regenerating intensity-modulated signals at 40 Gb/s [4]. More recent research advances indicated that all-optical 2R regeneration would also be achievable for phase-modulated [5], intensity-and-phase-modulated [6], and polarization-modulated [7] signals. Moreover, compared to their electronic counterparts (i.e., O/E/O 3R regenerators), all-optical 2R regenerators usually have compact sizes and relatively low power consumption [8]. Therefore, we expect them to be important building blocks for future optical transmission systems. Note that the technologies for all-optical 2R regeneration are still immature at this moment, and we therefore do not expect them to replace O/E/O 3R immediately. Previous research works have suggested that the energy efficiency of a translucent optical network can be further improved by leveraging the relatively low energy cost of all-optical 2R regenerators [9,10]. More specifically, while still satisfying the QoT constraint, we can partially replace some power-hungry O/E/O 3R regenerators with all-optical 2R regenerators and incorporate mixed regenerator placement (MRP) to reduce the energy cost [9].

Since a network element failure may lead to severe service disruptions in optical networks due to the high transmission rate, protection schemes have to be considered to provide resilience. Resilience in translucent optical networks has been investigated for both static [11–13] and dynamic [14,15] traffic scenarios. However, the resilience

Manuscript received December 17, 2012; revised May 24, 2013; accepted May 28, 2013; published June 28, 2013 (Doc. ID 181835).

Xiaoliang Chen, Fan Ji, Yanan Wu, and Zuqing Zhu (e-mail: zqzhu@ieee.org) are with the School of Information Science and Technology, University of Science and Technology of China, Hefei, Anhui 230027, China.

http://dx.doi.org/10.1364/JOCN.5.000741

schemes for the translucent networks using MRP have not been explored yet. Shared backup path protection (SBPP) is a path-based scheme that allocates two disjoint lightpaths to each connection as its working and protection paths, while the protection paths of multiple connections can share the same link resources if their working paths are disjoint [16,17]. One drawback of SBPP is that the backup resources can only be reserved but cannot be preconfigured [18], and this can incur relatively complicated signaling mechanisms and many switch reconfigurations during restoration, especially for the cases in which both working and protection paths consist of large numbers of hops. On the other hand, protection can also be realized with the link-based preconfigured-cycle (p-cycle) schemes [19–22]. In these schemes, a p-cycle is preconfigured to protect a working link, and, when the link fails, only its two end nodes engage in the restoration. Therefore, compared with SBPP, p-cycles can reduce the complexity of signaling mechanisms and switch reconfigurations. Moreover, previous work in [23,24] suggested that the relatively simple signaling mechanisms and few switch reconfigurations of p-cycles could lead to a shorter restoration time over SBPP. Nevertheless, since a p-cycle usually reserves the resources on more than one link to protect one link, it has an intrinsic drawback of low protection efficiency (PE).

In this paper, we investigate energy-efficient resilience for the translucent networks using MRP. We address both static and dynamic traffic scenarios and aim to provide 100% restoration against single-link failures while minimizing the total energy cost of regenerators. For static traffic, we first consider link-based protection using p-cycles and formulate an ILP model to solve the energy-efficient p-cycle design for translucent networks. The ILP model optimizes the allocation of working and protection resources jointly under the QoT constraint, with the objective to minimize the total energy cost. To reduce the computational complexity, we then propose a heuristic that can sequentially optimize the p-cycle designs for connections. For dynamic traffic, we first design an algorithm that can handle the setting up and tearing down of p-cycles dynamically, according to the time-variant connections. We enhance this algorithm afterward by introducing a p-cycle reoptimization procedure. An ILP model is formulated and solved for p-cycle reoptimization. In addition to the link-based p-cycle, we also study the path-based SBPP scheme.

The rest of the paper is organized as follows. With the static traffic scenario, Section II investigates the energy-efficient resilience designs for the translucent networks using MRP. Simulation results on the energy-efficient resilience designs for static traffic are presented in Section III. Section IV discusses the energy-efficient resilience designs for dynamic traffic, and Section V shows the corresponding simulation results. Finally, Section VI summarizes the paper.

II. Energy-Efficient Resilience in Translucent Networks with MRP and Static Traffic

Figure 1 illustrates an intuitive example of p-cycles in translucent networks with MRP. The working lightpath

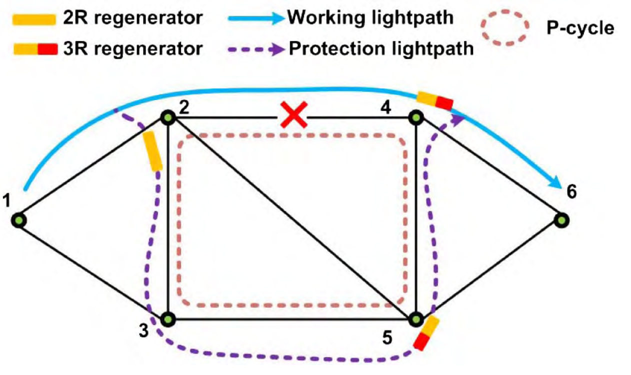

Fig. 1. Resilience based on a p-cycle in a translucent network with MRP.

(i.e., 1-2-4-6) passes through a 3R regenerator, which ensures the end-to-end QoT. For link 2-4, we construct a p-cycle (i.e., 2-3-5-4-2) and reserve corresponding wavelength and 2R/3R regenerator resources. When link 2-4 fails, we activate the rest of the cycle (i.e., 2-3-5-4) and reconfigure the optical switches on nodes 2 and 4 to reroute the working lightpath over 1-2-3-5-4-6 for restoration. Meanwhile, the MRP on the new route still ensures the end-to-end QoT. Similarly, we can construct p-cycles for links 1-2 and 4-6 and achieve 100% restoration against single-link failures. Moreover, note that the p-cycle 2-3-5-4-2 can also protect link 2-5 with segment 2-3-5, and protect link 5-2 with segment 5-4-2. In order to improve the energy efficiency of protection, we allow sharing of a p-cycle among multiple links.

The problem of energy-efficient resilience in translucent networks with MRP can be defined as follows. Given a network topology $G(V,E)$ and a traffic matrix Λ, we aim to perform routing and wavelength assignment (RWA) and MRP for working lightpaths and the corresponding p-cycles such that (1) the traffic between any source-destination pair in Λ can be served with working lightpaths that have sufficient end-to-end QoT, (2) the 100% restoration against single-link failures can be achieved with p-cycles, and (3) the total energy cost of all-optical 2R and O/E/O 3R regenerators is minimized.

A. ILP Formulation

We first formulate a joint ILP model to solve the working and protection resource allocations simultaneously for energy-efficient resilience in translucent networks with MRP. To reduce computational complexity, we perform the following precomputations: (1) For each s-d pair (s, $d \in V$) in $G(V,E)$, K shortest path candidates are calculated, denoted $\{R^k_{s,d}, k = 1, \ldots, K\}$; (2) all unidirectional cycles in $G(V,E)$ are found, denoted $\{C_i, i = 1, \ldots, N\}$, where N is the total number of cycles; and (3) for each routing path in $\{R^k_{s,d}\}$, $\forall s, d \in V, s \neq d$ or a unidirectional cycle C_i, a MRP solution is obtained with the minimum total energy cost while satisfying the QoT requirement [9].

In the context of this work, we evaluate the QoT of a lightpath with the end-to-end bit error rate (BER) and ensure that the end-to-end BER is below a preset threshold, denoted BER_t. Note that, in order to guarantee the QoT of restoration, we calculate MRP for a C_i according to the worst-case scenario, where the whole cycle would be utilized with a certain performance margin. The margin is reserved for a lightpath's transmission out of C_i. Moreover, during resilience design, we incorporate a step to validate the MRP of a p-cycle and make sure that the end-to-end BERs of all its restoration cases are below BER_t. We also assume that both 2R and 3R regenerators have wavelength conversion capability, and hence the wavelength continuity constraint holds only for the path segments between two regenerators. The joint ILP model is formulated as follows:

Notation:

- $G(V, E)$: Physical topology.
- W: Number of wavelengths on each fiber.
- Λ: Traffic matrix.
- $\lambda_{s,d}$: Traffic demand in Λ from s to d, s, $d \in V$.
- $l_{s,d,r}$: The r-th working lightpath from s to d.
- C_i: A unidirectional cycle in $G(V, E)$, where i is the unique ID.
- $R^k_{s,d}$: The k-th path candidate from s to d.
- P^j_R: Average energy cost per j-R regenerator ($j = 2, 3$).

Variables:

- $\chi_{i,e}$: Boolean variable that equals 1 if C_i can protect link e, $e \in E$, and 0 otherwise.
- ω_i: Integer variable that indicates the number of wavelengths being assigned to C_i.
- $f^{C,j}_{u,i}$: Boolean variable that equals 1 if a j-R regenerator is placed at node u in cycle C_i, and 0 otherwise.
- $f^{R,j}_{u,s,d,k}$: Boolean variable that equals 1 if a j-R regenerator is placed at node u in $R^k_{s,d}$, and 0 otherwise.
- $\psi_{r,s,d,k}$: Boolean variable that equals 1 if $l_{s,d,r}$ takes $R^k_{s,d}$, and 0 otherwise.
- $q^C_{i,e}$: Boolean variable that equals 1 if $e \in C_i$, and 0 otherwise.
- $q^R_{s,d,e,r}$: Boolean variable that equals 1 if $l_{s,d,r}$ routes over link e, and 0 otherwise.

Hence, the total regenerator energy cost of the resilience design for a translucent network with MRP is

$$P = \sum_i \omega_i \sum_{u \in C_i} \sum_{j=2}^{3} f^{C,j}_{u,i} \cdot P^j_R + \sum_{s,d} \sum_r \sum_k \psi_{r,s,d,k} \sum_{u \in R^k_{s,d}} \sum_{j=2}^{3} f^{R,j}_{u,s,d,k} \cdot P^j_R. \quad (1)$$

Objective:

$$\text{Minimize } P. \quad (2)$$

Constraints:

Equation (3) ensures that the wavelength assignment on each link e satisfies the capacity constraint:

$$\sum_i \omega_i \cdot q^C_{i,e} + \sum_{s,d} \sum_r q^R_{s,d,e,r} \le W, \quad \forall\, e \in E. \quad (3)$$

Equation (4) ensures single-path routing for each working lightpath $l_{s,d,r}$:

$$\sum_k \psi_{r,s,d,k} = 1, \quad \forall\, s, d, r. \quad (4)$$

Equation (5) ensures that the traffic demand is satisfied for each s-d pair in the traffic matrix:

$$\sum_r \sum_k \psi_{r,s,d,k} \ge \lambda_{s,d}, \quad \forall\, s, d. \quad (5)$$

Equations (6) and (7) ensure that at most one regenerator is allocated at node u for each wavelength channel of a p-cycle or a working lightpath:

$$\sum_j f^{C,j}_{u,i} \le 1, \quad \forall\, u, i, \quad (6)$$

$$\sum_j f^{R,j}_{u,s,d,k} \le 1, \quad \forall\, u, s, d, k. \quad (7)$$

Equation (8) ensures that all working lightpaths are protected by the p-cycles and 100% restoration can be achieved against single-link failures:

$$\sum_i \omega_i \cdot \chi_{i,e} \ge \sum_{s,d} \sum_r q^R_{s,d,e,r}, \quad \forall\, e \in E. \quad (8)$$

Equation (9) limits the ranges of the variables:

$$\omega_i \in [0, W], \quad \chi_{i,e}, f^{C,j}_{u,i}, f^{R,j}_{u,s,d,k}, \psi_{r,s,d,k}, q^C_{i,e}, q^R_{s,d,e,r} \in \{0, 1\}. \quad (9)$$

We obtain the working lightpaths, the p-cycles, and the associated MRP by solving the joint ILP, and then assign wavelengths accordingly under the wavelength continuity constraint. For this static traffic scenario, we assume that the wavelength resource is sufficient (i.e., W is sufficiently large) for the traffic demands, and we do not consider request blocking.

B. Heuristic Algorithm

The joint ILP can provide the optimal resilience design with the highest energy efficiency. However, its computational complexity is also high, which determines that it is not scalable with the network scale or the traffic volume. In this subsection, we discuss a heuristic algorithm that handles the designs of the working lightpaths and p-cycles separately for high computational efficiency.

Definition: The PE of a backup structure is the proportion of the working wavelength capacity it can protect relative to the capacity it actually occupies.

Algorithm 1 explains the details of the heuristic, which has two phases. In the first phase, working lightpaths are set up using the shortest path routing and the energy-efficient MRP scheme developed in [9], and then the wavelength assignment is performed based on the maximum transparent segment scheme [25]. In the second phase, p-cycles are assembled iteratively, based on their PEs, from high to low, until all working lightpaths are protected against single-link failures.

Algorithm 1: Energy-Efficient Resilience Design for Translucent Networks With MRP and Static Traffic

{Phase I: Setting up working lightpaths}
for *all* $\lambda_{s,d} \in \Lambda$ **do**
    decompose $\lambda_{s,d}$ into $\{l_{s,d,r}\}$ based on the capacity of a wavelength channel;
    for *all* $\{l_{s,d,r}\}$ *of the current s-d pair* **do**
        find the shortest path from s to d in $G(V,E)$;
        obtain energy-efficient MRP along the path [9];
        assign wavelengths with minimum additional wavelength conversions [25];
    end
end
{Phase II: Assembling p-cycles}
calculate all unidirectional cycles $\{C_i\}$ in $G(V,E)$;
obtain energy-efficient MRP for each C_i;
While *there is working capacity not protected yet* **do**
    calculate PE for each C_i based on the working capacity that is not yet protected;
    select the C_i that has the highest PE;
    assign wavelengths for the C_i with minimum additional wavelength conversions;
    subtract the capacity that C_i can protect from the outstanding working capacity;
end

III. Simulation Results for Static Traffic Scenario

In order to evaluate the performance of the resilience design algorithms discussed in the previous section, we perform simulations using the NSFNET topology in Fig. 2. For the topology, we define two types of nodes: (1) switching nodes (labeled with numbers) where the lightpaths can start and end and (2) by-pass regeneration sites where the lightpaths can only pass through. We assume that the link length between two by-pass regeneration sites is

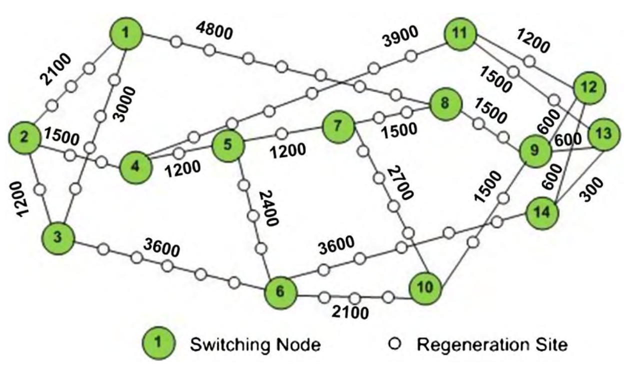

Fig. 2. NSFNET topology for simulations.

identical: 600 km. With this topology, we obtain 252 unidirectional cycles using the algorithm developed in [26]. The average energy costs of 2R and 3R regenerators (i.e., P_R^2 and P_R^3) are assumed to be 2 and 15 units, respectively, according to the experimental results in [8]. The datarate of each wavelength channel is set as 40 Gbits/s, and the QoT threshold of each lightpath is $\mathrm{BER}_t = 10^{-4}$ to accommodate the forward-error-correction (FEC) threshold. Other physical parameters for QoT estimations are the same as those in [9]. In the simulations, we compare three energy-efficient resilience design algorithms, i.e., the p-cycle design with ILP (p-cycle-ILP), the p-cycle design with the heuristic (p-cycle-HEU), and the SBPP design with the algorithm in [27]. We consider both uniform and nonuniform traffic distributions. For the uniform case, the traffic demands are generated by randomly selecting their *s-d* pairs in the topology. We use the traffic matrix in Table I, which is from a realistic traffic analysis [28], for the nonuniform case. We use GLPK [29] to solve the ILPs, and use MATLAB to implement the heuristic.

Figures 3 and 4 show the simulation results for static uniform traffic. Figure 3(a) compares the total energy costs from the three algorithms for different traffic volumes. It can be seen that when the total network throughput is ≤16 Tbits/s, the energy cost from p-cycle-HEU is close to that from p-cycle-ILP. However, when the traffic volume keeps increasing, the designs from p-cycle-HEU require more extra energy when compared with those from p-cycle-ILP. This is because p-cycle-ILP optimizes the energy costs for all traffic demands jointly, and its advantage over p-cycle-HEU that handles the demands sequentially increases dramatically with the number of demands, i.e., the traffic volume. On average, the resilience designs from p-cycle-HEU consume 16.6% extra energy than those from p-cycle-ILP. When comparing the p-cycle schemes with SBPP, we observe that SBPP consumes less energy than p-cycle. This is because the p-cycle schemes usually reserve the resources on more than one link to protect one link, which leads to relatively long restoration paths. On average, the solutions from p-cycle-ILP consume 21.87% extra energy than those from SBPP. Figure 3(b) illustrates the average wavelength usage per link from the algorithms, which indicates that p-cycle-HEU requires 21.1% more wavelength channels on average than the p-cycle-ILP. Compared with p-cycle-ILP, SBPP provides similar results on wavelength usage per link, while the results from p-cycle-HEU are the highest.

Figure 4 shows the simulation results on average PE per p-cycle. It can be seen that the PE from p-cycle-ILP is higher than that from p-cycle-HEU and increases with the traffic volume. This is because p-cycle-ILP optimizes the resilience designs for all lightpaths jointly. Therefore, when traffic volume increases, the possibility of p-cycles sharing also becomes larger, and this eventually pushes the average PE from p-cycle-ILP to go higher. However, for p-cycle-HEU, it optimizes the resilience designs for the lightpaths sequentially and cannot achieve the global optimum, and thus its average PE stays almost unchanged for different traffic volumes. The overall average PE from p-cycle-ILP is 1.33, while it is 0.75 for p-cycle-HEU.

TABLE I
TRAFFIC MATRIX Λ FOR NONUNIFORM TRAFFIC DISTRIBUTION

Node	1	2	3	4	5	6	7	8	9	10	11	12	13	14
1	0	2	1	1	1	4	1	1	2	1	1	1	1	1
2	2	0	2	1	8	2	1	5	3	5	1	5	1	4
3	1	2	0	2	3	2	11	20	5	2	1	1	1	2
4	1	1	2	0	1	1	2	1	2	2	1	2	1	2
5	1	8	3	1	0	3	3	7	3	3	1	5	2	5
6	4	2	2	1	3	0	2	1	2	2	1	1	1	2
7	1	1	11	2	3	2	0	9	4	20	1	8	1	4
8	1	5	20	1	7	1	9	0	27	7	2	3	2	4
9	2	3	5	2	3	2	4	27	0	75	2	9	3	1
10	1	5	2	2	3	2	20	7	75	0	1	1	2	1
11	1	1	1	1	1	1	1	2	2	1	0	2	1	61
12	1	5	1	2	5	1	8	3	9	1	2	0	1	81
13	1	1	1	1	2	1	1	2	3	2	1	1	0	2
14	1	4	2	2	5	2	4	4	0	1	61	81	2	0

Figures 5 and 6 show the simulation results for static nonuniform traffic. For the regenerator energy cost and wavelength usage, similar trends can be seen. According to Table I, most of the traffic is distributed between nodes that are adjacent in the network, and thus the total energy costs in Fig. 5(a) are lower than those in Fig. 3(a). For the results on average PE, we can see that the values are lower than those for the uniform traffic case. The overall average PE from p-cycle-ILP is 0.90, while it is 0.60 for p-cycle-HEU. This is because, compared with uniform traffic, different working lightpaths have a larger possibility to share links with nonuniform traffic. Therefore, in order to protect against single-link failures, the algorithm needs to assemble more p-cycles, even when the network traffic volume is the same.

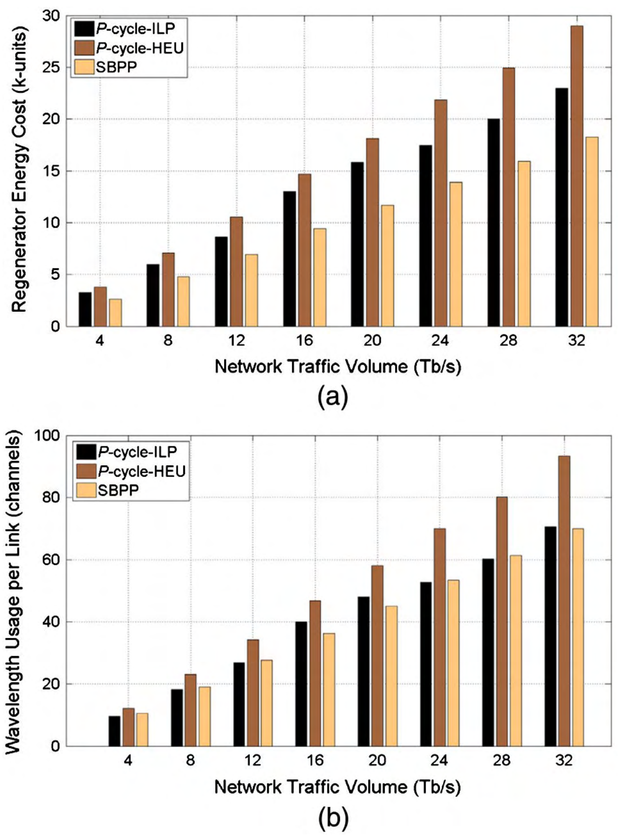

Fig. 3. Simulation results for static uniform traffic: (a) Total regenerator energy cost and (b) average wavelength usage per link.

IV. ENERGY-EFFICIENT RESILIENCE IN TRANSLUCENT NETWORKS WITH MRP AND DYNAMIC TRAFFIC

The static traffic scenario is usually used for the network planning phase, where network operators scale networks with traffic predictions. However, for practical network operations, network operators also need to handle dynamic traffic; i.e., the lightpath requests are time variant and can arrive and leave on the fly. In this section, we investigate resilience designs for translucent networks with MRP and dynamic traffic.

Since it would be difficult to adjust network resources (i.e., number of wavelength channels per link W and number of available 2R and 3R regenerators in each node) on the fly in dynamic network operations [30], we assume that the network resources are predetermined according to a link budget and an energy budget. Consequently, we need to consider request blocking, when a feasible working

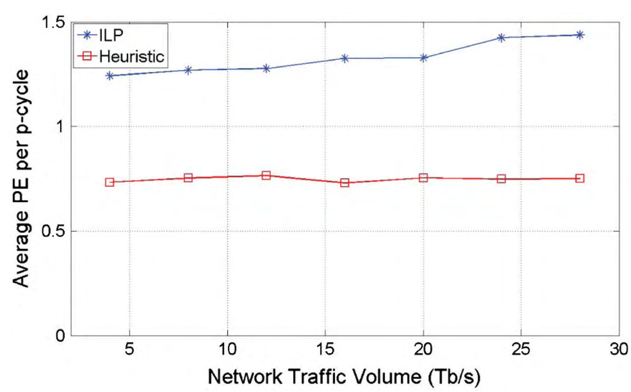

Fig. 4. Simulation results on average PE per p-cycle for static uniform traffic.

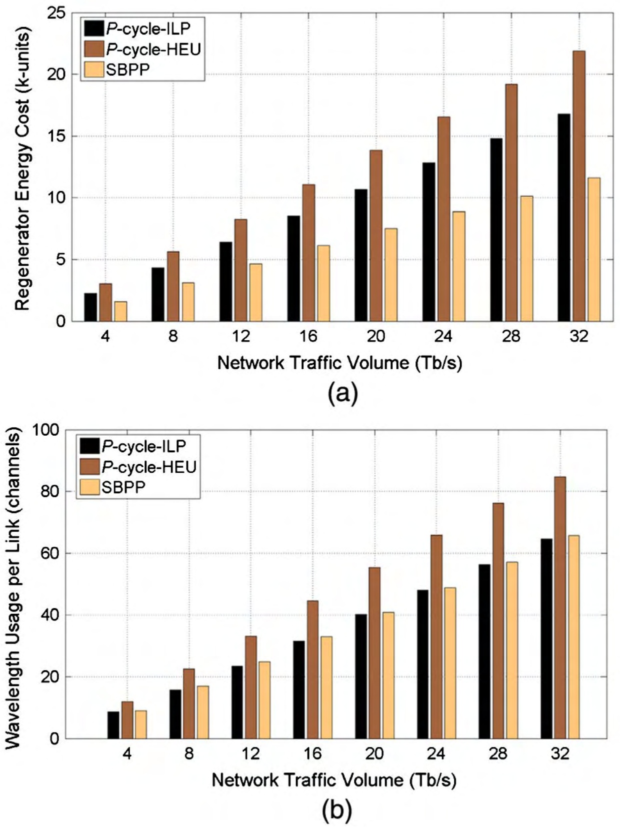

Fig. 5. Simulation results for static nonuniform traffic: (a) Total regenerator energy cost and (b) average wavelength usage per link.

lightpath and the associated protection cannot be found for a request under the resource constraints. The objective of the dynamic resilience design is to jointly minimize the number of blocked requests and the regenerator energy cost.

A. Resilience With p-Cycle

We first consider a dynamic resilience design algorithm that is modified from Algorithm 1, and call it *p*-cycle design without reoptimization (*p*-cycle-NRO). When a dynamic

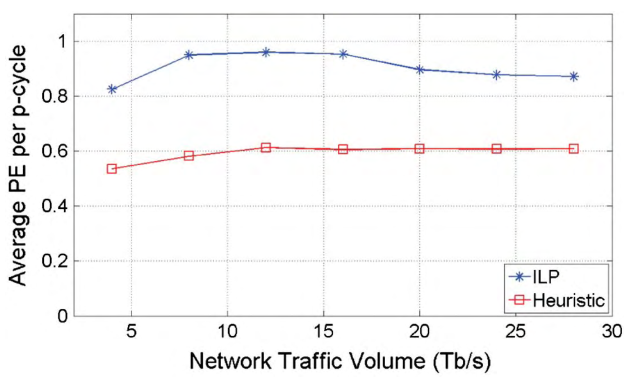

Fig. 6. Simulation results on average PE per *p*-cycle for static nonuniform traffic.

lightpath request arrives, *p*-cycle-NRO serves it with the shortest path between its *s*-*d* pair, and allocates available wavelengths and proper regenerators along the path. Then the algorithm checks whether the existing *p*-cycles in the network can protect it; otherwise, additional *p*-cycles are assembled according to their PEs in descending order until the lightpath is protected against single-link failures. If any of the above procedures fails, the request is blocked. Unnecessary *p*-cycles, i.e., those that do not protect any working lightpath anymore, are dismantled when the requests have expired.

To further improve the energy efficiency of dynamic resilience design with MRP, we introduce a reoptimization procedure to reassemble the existing *p*-cycles in the network. Note that, as all working lightpaths remain untouched during the reoptimization, this procedure does not cause any service interruption. We formulate an ILP model to solve the reoptimization with minimum backup energy cost.

Notation:

- $G(V,E)$: Physical topology.
- W: Number of wavelengths on each fiber.
- C_i: A unidirectional cycle in $G(V,E)$, where i is the unique ID.
- P_R^j: Average energy cost per j-R regenerator ($j=2,3$).
- $N_u^{R,j}$: Number of available j-R regenerators in node u.
- D_e: Number of working lightpaths on link e.

Variables:

- $\chi_{i,e}$: Boolean variable that equals 1 if C_i can protect link e, $e \in E$, and 0 otherwise.
- ω_i: Integer variable that indicates the number of wavelengths being assigned to C_i.
- $f_{u,i}^{C,j}$: Boolean variable that equals 1 if a j-R regenerator is placed at node u in cycle C_i, and 0 otherwise.
- $q_{i,e}^{C}$: Boolean variable that equals 1 if $e \in C_i$, and 0 otherwise.

Hence, the total regenerator energy cost of the *p*-cycles in the network is

$$P_{\text{backup}} = \sum_i \omega_i \sum_{u \in C_i} \sum_{j=2}^{3} f_{u,i}^{C,j} \cdot P_R^j. \tag{10}$$

For the reoptimization, we have

Objective:

$$\text{Minimize } P_{\text{backup}}. \tag{11}$$

Constraints:

Equation (12) ensures that the wavelength assignment on each link e satisfies the capacity constraint:

$$\sum_i \omega_i \cdot q_{i,e}^{C} + D_e \leq W, \quad \forall\, e \in E. \tag{12}$$

Equation (13) ensures that all working lightpaths are still protected by the new *p*-cycles:

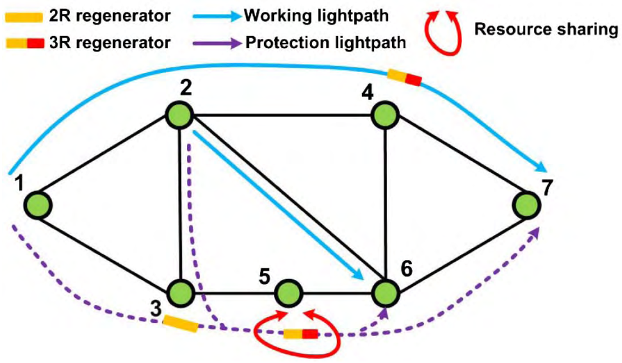

Fig. 7. Resilience based on SBPP in a translucent network with MRP.

$$\sum_i \omega_i \cdot \chi_{i,e} \geq D_e, \quad \forall\, e \in E. \tag{13}$$

Equation (14) ensures that the regenerator allocation satisfies the regenerator resource constraint:

$$\sum_i \omega_i \cdot f_{u,i}^{C,j} \leq N_u^{R,j}, \quad \forall\, u \in V, \quad \forall\, j \in \{2,3\}. \tag{14}$$

Equation (15) limits the ranges of the variables:

$$\omega_i \in [0, W], \chi_{i,e}, f_{u,i}^{C,j}, q_{i,e}^{C} \in \{0,1\}. \tag{15}$$

By solving the ILP, we obtain the cycle selection, the wavelength assignment, and the regenerator allocation of new p-cycles that can protect current working lightpaths against single-link failures, with the minimum energy cost. For the timing, we consider two scenarios: (1) on demand and (2) on schedule. For the p-cycle design with on demand reoptimization (p-cycle-oDRO), we invoke a reoptimization whenever a request cannot be served. However, for the p-cycle design with on schedule reoptimization (p-cycle-oSRO), we invoke a reoptimization with a fixed operation time interval.

B. Resilience With Shared Backup Path Protection (SBPP)

For dynamic resilience design, we also consider SBPP. SBPP ensures that each working lightpath is protected by a backup one, while different backup paths can share the same resources as long as their working paths are disjoint. Figure 7 shows an example of SBPP in a translucent network with MRP. We can see that the backup paths of disjoint lightpaths 1-2-4-7 and 2-6 traverse links 3-5 and 5-6, and thus they can share the resources on nodes 3 and 5 and links 3-5 and 5-6.

Algorithm 2 shows the detailed procedures of dynamic resilience design with SBPP. When a lightpath request

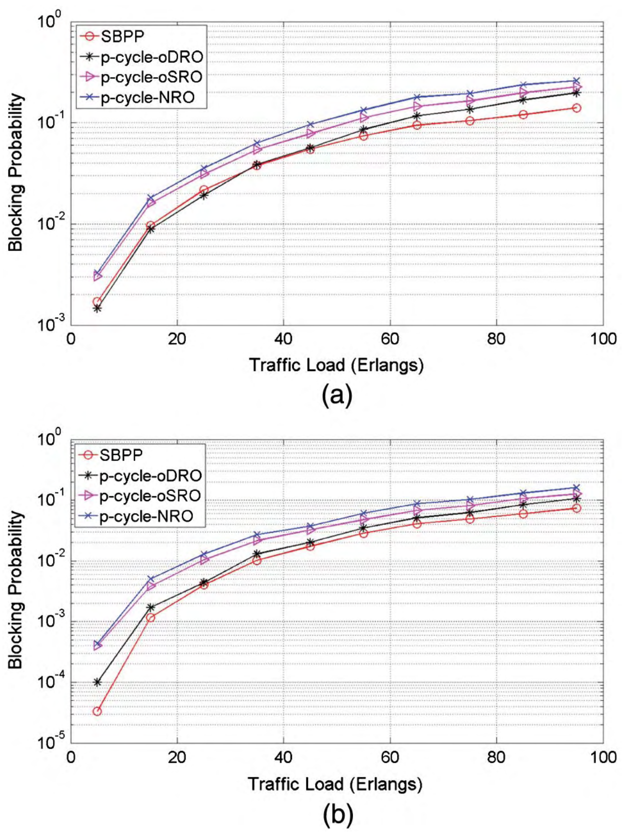

Fig. 8. Blocking probability versus traffic load from different dynamic resilience design algorithms: (a) Total energy budget is 15 k units and (b) total energy budget is 20 k units.

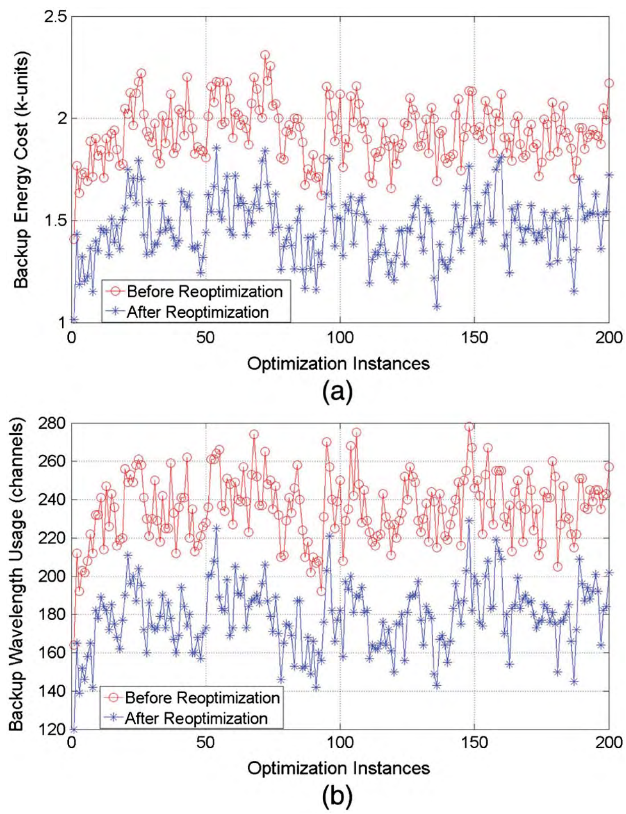

Fig. 9. Comparisons of (a) backup energy cost and (b) backup wavelength usage, before and after reoptimization with p-cycle-oSRO and the total energy budget of 15 k units.

arrives, we calculate two disjoint shortest paths for its *s*-*d* pair and use the shorter one as the working path. After allocating wavelength channels and regenerators along the working path, we check each link of the backup path and determine whether it can share resources with any existing backup path. New wavelengths and regenerators are allocated if resource sharing is not feasible; otherwise, we update the resource sharing information and reallocate regenerators if necessary.

Algorithm 2: Dynamic Resilience Design With SBPP

While *network is operational* **do**
  restore network resources used by expired requests;
  for *each new request* **do**
    get the shortest path $R^1_{s,d}$ of the *s*-*d* pair;
    assign working lightpath to $R^1_{s,d}$;
    obtain energy-efficient MRP along $R^1_{s,d}$ [9];
    assign wavelengths with minimum additional wavelength conversions [25];
    If *working path provisioning is successful* **then**
      remove links $e \in R^1_{s,d}$ in $G(V,E)$;
      get the shortest path $R^2_{s,d}$ in $G(V,E)$;
      assign backup path to $R^2_{s,d}$;
      for *each link* $e \in R^2_{s,d}$ **do**
        If *e can be shared with other backup path(s)* **then**
          re-allocate regenerator(s) if necessary;
          update resource sharing information;
        else
          perform wavelength assignment and regenerator allocation;
        end
      end
      If *backup path provisioning is success* **then**
        mark the request as provisioned;
      else
        mark the request as blocked;
      end
    else
      mark the request as blocked;
    end
  end
end

V. Simulation Results for Dynamic Traffic Scenario

In this section, we discuss simulation results for dynamic resilience designs for translucent networks with MRP. We still use the NSFNET topology in Fig. 2 and assume that each link accommodates 40 wavelength channels. We fix the total energy cost budget as 15 and 20 k units and distribute the 2R and 3R regenerators evenly in the nodes. The *s*-*d* pairs of the dynamic requests are randomly chosen, i.e., the dynamic traffic is uniform. The requests' arrivals follow a Poisson process with an average rate of λ requests per time unit, and the lifetime of each request follows the negative exponential distribution with an average of $1/\mu$ time units. Hence, the traffic load can be quantified with λ/μ in Erlangs. The rest of the simulation parameters are the same as those in Section III.

Figure 8 plots the blocking probability from different dynamic resilience design algorithms. As a path-based scheme, SBPP is interstitially more capacity efficient than the link-based *p*-cycle, with a much longer restoration time [18]. Therefore, when the energy budget is the same, SBPP achieves the best blocking performance for almost all traffic scenarios in Fig. 8, especially when the load is heavy. For SBPP, when adjacent links along a backup path are shared by different working lightpaths, the corresponding intermediate nodes need to be reconfigured during restoration, in addition to the source and destination nodes. Our simulations indicate that the average number of reconfigurations per restoration for SBPP is 3.75. For a *p*-cycle scheme, we only need to reconfigure the two end nodes of a failed link per restoration, and thus its number of reconfigurations is always 2.

Among the *p*-cycle schemes, *p*-cycle-oDRO provides the lowest blocking probabilities. The blocking performance of *p*-cycle-oDRO is close to that of SBPP and is even slightly better when the traffic load is ≤40 Erlangs in Fig. 8(a). The blocking performance of *p*-cycle-oSRO falls in between those of *p*-cycle-oDRO and *p*-cycle-NRO, which reveals the trade-off between blocking performance and

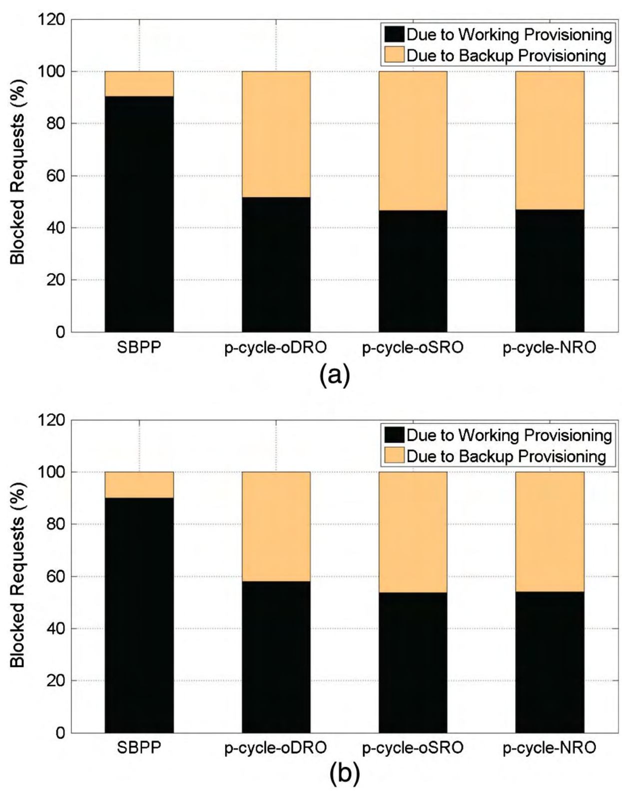

Fig. 10. Distributions of request blocking reasons for different dynamic resilience design algorithms: (a) Total energy budget is 15 k units and (b) total energy budget is 20 k units.

operation complexity. Figure 9 compares the backup energy cost and the backup wavelength usage before and after reoptimization for p-cycle-oSRO with the total energy budget of 15 k units. We can see that both the energy and wavelength channels consumed by the p-cycles decrease dramatically after the reoptimizations. To further analyze the performance of the proposed algorithms, we investigate the reasons that caused request blocking, and Fig. 10 shows the results. For SBPP, the majority of request blockings ($> 90\%$) are due to the failures of working lightpath provisioning, while the backup paths can be assembled smoothly due to the effective resource sharing. For the p-cycle schemes, backup provisioning causes more request blockings because the backup paths consume more resources.

VI. Conclusion

We studied energy-efficient resilience designs for translucent optical networks using MRP. We considered both static and dynamic traffic scenarios and aimed to provide 100% restoration against single-link failures while minimizing the total energy-cost on regenerators. For static traffic scenarios, we formulated an ILP model to optimize the allocation of working and protection resources jointly under the QoT constraint and proposed a heuristic that can sequentially optimize the p-cycle designs for connections. Simulations evaluated the performance of the algorithms with both uniform and nonuniform traffic models. For dynamic traffic scenarios, we designed three algorithms for p-cycle designs and also investigated the SBPP scheme. The simulation results of dynamic traffic scenarios indicated that when the energy budget was fixed, the SBPP scheme could achieve the lowest blocking probability because of its high-capacity efficiency. However, for the p-cycle schemes, the simulation results verified that reoptimization could effectively reduce blocking probability. The results also showed that the blocking performance of p-cycle-oDRO was the lowest among three p-cycle based dynamic resilience design algorithms.

Acknowledgments

This work was supported in part by the Program for New Century Excellent Talents in University (NCET) under Project NCET-11-0884 and the Natural Science Foundation of Anhui Province under Project 1208085MF88.

References

[1] *Cisco Visual Networking Index: Forecast and Methodology, 2011–2016*, Cisco, 2011.

[2] B. Ramamurthy, H. Feng, D. Datta, J. P. Heritage, and B. Mukherjee, “Transparent vs. opaque vs. translucent wavelength-routed optical networks,” in *Optical Fiber Communication Conf. and the Int. Conf. on Integrated Optics and Optical Fiber Communication*, 1999, paper TuF2.

[3] Z. Zhu, M. Funabashi, P. Zhong, L. Paraschis, D. Harris, and S. Yoo, “High-performance optical 3R regeneration for scalable fiber transmission system applications,” *J. Lightwave Technol.*, vol. 25, pp. 504–511, Feb. 2007.

[4] G. Maxwell, B. Manning, M. Nield, M. Hariow, C. Ford, M. Clements, S. Lucas, P. Townley, R. McDougall, S. Oliver, R. Cecil, L. Johnston, A. Poustie, R. Webb, I. Lealman, L. Rivers, J. King, S. Perrin, R. Moore, I. Reid, and D. Scrase, “Very low coupling loss, hybrid-integrated all-optical regenerator with passive assembly,” in *28th European Conf. on Optical Communication (ECOC)*, Sept. 2002, vol. 2, pp. 1–2.

[5] K. N. Nguyen, T. Kise, J. M. Garcia, H. Poulsen, and D. J. Blumenthal, “All-optical 2R regeneration of BPSK and QPSK data using a 90° optical hybrid and integrated SOA-MZI wavelength converter pairs,” in *Optical Fiber Communication Conf. and the Nat. Fiber Optic Engineers Conf.*, 2011, paper OMT3.

[6] X. Yi, R. Yu, J. Kurumida, and B. Yoo, “A theoretical and experimental study on modulation-format-independent wavelength conversion,” *J. Lightwave Technol.*, vol. 28, pp. 587–595, Feb. 2010.

[7] N. Andriolli, S. Faralli, X. Leijtens, J. Bolk, and G. Contestabile, “Monolithically integrated all-optical regenerator for constant envelope WDM signals,” *J. Lightwave Technol.*, vol. 31, pp. 322–327, Jan. 2013.

[8] O. Leclerc, B. Lavigne, E. Balmefrezol, P. Brindel, L. Pierre, D. Rouvillain, and F. Seguineau, “Optical regeneration at 40 Gb/s and beyond,” *J. Lightwave Technol.*, vol. 21, pp. 2779–2790, Nov. 2003.

[9] Z. Zhu, X. Chen, F. Ji, L. Zhang, F. Farahmand, and J. Jue, “Energy-efficient translucent optical transport networks with mixed regenerator placement,” *J. Lightwave Technol.*, vol. 30, pp. 3147–3156, Oct. 2012.

[10] A. N. Patel, P. N. Ji, A. Nag, Y.-K. Huang, E. Ip, R. Chandrasekaran, and J. P. Jue, “Optimal placement of combined 2R/3R regenerators in WDM networks,” in *17th Opto-Electronics and Communications Conf. (OECC)*, July 2012, pp. 429–430.

[11] H. Zang, R. Huang, and J. Pan, “Methodologies on designing a hybrid shared-mesh-protected WDM network with sparse wavelength conversion and regeneration,” *Proc. SPIE*, vol. 4910, pp. 188–196, Oct. 2002.

[12] X. Yang, L. Shen, and B. Ramamurthy, “Survivable lightpath provisioning in WDM mesh networks under shared path protection and signal quality constraints,” *J. Lightwave Technol.*, vol. 23, pp. 1556–1567, Apr. 2005.

[13] B. Chatelian, S. Mannor, F. Gagnon, and D. Plant, “Non-cooperative design of translucent networks,” in *IEEE Global Telecommunications Conf. (GLOBECOM)*, Nov. 2007, pp. 2348–2352.

[14] Y. Ouyang, Q. Zeng, and W. Wei, “Dynamic lightpath provisioning with signal quality guarantees in survivable translucent optical networks,” *Opt. Express*, vol. 13, pp. 10457–10468, Dec. 2005.

[15] N. Sambo, I. Cerutti, F. Cugini, A. Giorgetti, L. Valcarenghi, and P. Castoldi, “Segment restoration scheme with QoT-guarantees in GMPLS-controlled translucent networks,” in *34th European Conf. on Optical Communication (ECOC)*, Sept. 2008, pp. 1–2.

[16] S. Ramamurthy and B. Mukherjee, “Survivable WDM mesh networks. Part I—protection,” in *18th Annu. Joint Conf. of the IEEE Computer and Communications Societies (IEEE INFOCOM)*, Mar. 1999, pp. 744–751.

[17] E. Bouillet, G. Ellinas, J.-F. Labourdette, and R. Ramamurthy, *Path Routing in Mesh Optical Networks*. Chichester: Wiley, 2007.

[18] S. Ramamurthy, L. Sahasrabuddhe, and B. Mukherjee, "Survivable WDM mesh networks," *J. Lightwave Technol.*, vol. 21, pp. 870–883, Apr. 2003.

[19] W. Grover and D. Stamatelakis, "Cycle-oriented distributed preconfiguration: Ring-like speed with mesh-like capacity for self-planning network restoration," in *IEEE Int. Conf. on Communications (ICC)*, June 1998, vol. 1, pp. 537–543.

[20] D. Schupke, C. Gruber, and A. Autenrieth, "Optimal configuration of *p*-cycles in WDM networks," in *IEEE Int. Conf. on Communications (ICC)*, June 2002, vol. 5, pp. 2761–2765.

[21] Z. Zhang, W. Zhong, and B. Mukherjee, "A heuristic method for design of survivable WDM networks with *p*-cycles," *IEEE Commun. Lett.*, vol. 8, pp. 467–469, July 2004.

[22] A. Eshoul and H. Mouftah, "Survivability approaches using *p*-cycles in WDM mesh networks under static traffic," *IEEE/ACM Trans. Netw.*, vol. 17, pp. 671–683, Apr. 2009.

[23] L. Sahasrabuddhe, S. Ramamurthy, and B. Mukherjee, "Fault management in IP-over-WDM networks: WDM protection versus IP restoration," *IEEE J. Sel. Areas Commun.*, vol. 20, pp. 21–33, Jan. 2002.

[24] W. He and A. Somani, "Comparison of protection mechanism: Capacity efficiency and recovery time," in *IEEE Int. Conf. on Communications (ICC)*, June 2007, pp. 2218–2223.

[25] Z. Zhu, W. Zhong, and C. Wan, "Joint optimization of mixed regenerator placement and wavelength assignment for green translucent optical networks," in *Asia Communications and Photonics Conf. and Exhibition (ACP)*, Nov. 2011, pp. 1–6.

[26] A. Eshoul and H. T. Mouftah, "Performance evaluation of dynamic *p*-cycle protection methods in WDM optical networks," in *11th Int. Conf. on Transparent Optical Networks (ICTON)*, July 2009, pp. 1–4.

[27] X. Chen, F. Ji, and Z. Zhu, "Energy-efficient protection designs for translucent optical networks using mixed regenerator placement," in *Optical Fiber Communication Conf.*, 2013, paper JTh2A.63.

[28] A. Nag, M. Tornatore, and B. Mukherjee, "Optical network design with mixed line rates and multiple modulation formats," *J. Lightwave Technol.*, vol. 28, pp. 466–475, Feb. 2010.

[29] GLPK (GNU Linear Programming Kit), http://www.gnu.org/software/glpk/.

[30] B. Mukherjee, *Optical WDM Networks*. Berlin: Springer, 2006.

Xiaoliang Chen received the B.S. degree from the Department of Electrical Engineering, North University of China, Taiyuan, China, in 2011. He is working toward his M.S. degree at the School of Information Science and Technology, University of Science and Technology of China, Hefei, China. His research interest is energy-efficient optical networks.

Fan Ji received the B.S. degree from the Department of Electrical Engineering, Hainan University, Haikou, China, in 2012. She is working toward her M.S. degree at the School of Information Science and Technology, University of Science and Technology of China, Hefei, China. Her research interest is elastic optical networks.

Yanan Wu received the B.S. degree from the Department of Electrical Engineering, Nanjing University of Aeronautics and Astronautics, Nanjing, China, in 2011. She is working toward her M.S. degree at the School of Information Science and Technology, University of Science and Technology of China, Hefei, China. Her research interest is energy-efficient networks.

Zuqing Zhu (M'07-SM'12) received the Ph.D. degree from the Department of Electrical and Computer Engineering, University of California, Davis, in 2007. From July 2007 to January 2011, he worked in the Service Provider Technology Group of Cisco Systems, San Jose, as a senior R&D engineer. In January 2011, he joined the University of Science and Technology of China (USTC), where he currently is an Associate Professor. His research interests are optical networks, energy-efficient networks, and cloud computing. He has published more than 80 papers in peer-reviewed journals and conferences of IEEE, IEE, and OSA. He has been in the technical program committee (TPC) of INFOCOM, ICC, GLOBECOM, ICCCN, etc. He was a guest editor of the *IEEE Network* special issue on "Optical Networks in Cloud Computing." He is also an editorial board member of Elsevier's *Journal of Optical Switching and Networking* (OSN), Springer's *Telecommunication Systems Journal* (TSMJ), Wiley's *European Transactions on Emerging Telecommunications Technologies* (ETT), etc. He is a Senior Member of IEEE and a Member of OSA.